

# ACHIEVABLE THROUGHPUT WITH BLOCK DIAGONALIZATION ON OFDM INDOOR DEMONSTRATOR

*M. Morales Céspedes, A. García Armada\**

*J. Gutiérrez Terán*

Dept. of Signal Theory and Communications  
University Carlos III of Madrid, Leganés, Spain  
Email: {maximo, agarcia}@tsc.uc3m.es

Dept. of Communications Engineering  
University of Cantabria, Santander, Spain  
Email: jesugt@gtas.dicom.unican.es

## ABSTRACT

Block Diagonalization (BD) is a linear precoding transmission technique able to achieve full multiplexing gain in multiple antenna systems. In this work we present a Multiple-Input Multiple-Output (MIMO) implementation based on Orthogonal Frequency Division Multiplexing (OFDM) made up of a transmitter with 4 antennas and 2 users equipped with 2 antennas each one, which allows us to evaluate the performance of BD in indoor scenarios. First, the theoretic achievable rates are obtained for the measured channel in an offline evaluation. After that, the bit error rate performance is evaluated regarding the system sum throughput. To the best of our knowledge, this is the first time that BD performance is validated using a multiuser MIMO testbed.

**Index Terms**— Multiple-Input Multiple Output (MIMO) testbed; Orthogonal Frequency Division Multiplexing (OFDM); interference channel; block diagonalization (BD)

## 1. INTRODUCTION

Multiple Input Multiple Output (MIMO) systems emerged as a means of achieving high capacity communications. In recent years, low complexity coordinated base station transmission (CBST) alternatives such as Zero Forcing (ZF) [1], Block Diagonalization (BD) [2] or Interference Alignment (IA) [3], which exploit the available spatial degrees of freedom have been developed. Unfortunately these approaches require an accurate channel state information at the transmitter (CSIT). This issue involves a high quality and instantaneous feedback between users and transmitters that is hard to achieve in real implementations. The effects of a limited feedback on BD for the MIMO broadcast channel are analyzed in [4]. This work shows a rate gap between BD and ZF which increases under limited feedback due to the dimensionality advantage.

To understand the impact of these techniques on practical wireless networks, it is necessary to evaluate their performance in real scenarios beyond simple channel models of-

ten used in simulation-based approaches (e.g. spatially uncorrelated channels, perfect synchronization, channel coding...). However, due to the cost associated to the required hardware set-up, the literature about ZF, BD or IA real implementations is scarce. In [5] a experimental study of IA focused on MIMO-OFDM 3-user interference channel demonstrates that the performance obtained in software simulations is achievable in a real implementation. The main limitation of this work relies on that the obtained results are based on measured channels and a subsequent offline evaluation. Hence, practical issues such as synchronization or hardware impairments are not taken into account. A study of IA performance focused on 3-user interference wireless channel is presented in [6]. This work identifies the main practical issues that affect the IA performance in a real implementation, concluding that imperfect CSIT is the key limiting factor. The achievable rate for ZF technique in a 2 transmitters and 2 users equipped with one antenna each testbed is presented in [7].

In this paper we present BD experiments in the 5 GHz band carried out with a MIMO-OFDM testbed [8]. This testbed builds an indoor 2-user wireless channel where each user is equipped with 2 receive antennas and the transmitter is made up by 4 antennas. Under this scenario BD achieves two data streams per user. The aim of this paper is to demonstrate the achievable throughput using BD and show the advantage of this technique over ZF in a real implementation. The conducted experiments comprise two steps; a training stage where each user receives a pilot frame from each transmit antenna; and a data transmission stage composed by a simultaneous transmission phase implementing BD, and a sequential phase which is used as a benchmark for comparison purposes.

## 2. SYSTEM MODEL

The system model assumes a downlink broadcast transmission scenario based on OFDM. The transmitter is equipped with  $t$  antennas serving  $N$  users equipped with  $r$  antennas each. Assuming flat frequency response in each subcarrier, the channel can be modeled by a set of  $Nr \times t$  channel matri-

\*This work has been partially funded by research projects COMONSENS (CSD2008-00010), and GRE3N (TEC2011-29006-C03-02).

ces  $\mathbf{H} = \{\mathbf{H}^1, \mathbf{H}^2, \dots, \mathbf{H}^p, \dots, \mathbf{H}^{N_{ofdm}}\}$  where each coefficient represents the channel response between a given transmitter antenna and a given receive antenna at each user on the  $p$ -th subcarrier. The received signal model is as follows

$$\mathbf{y}^p = \mathbf{H}^p \mathbf{x}^p + \mathbf{n}^p, \quad (1)$$

where  $\mathbf{y}^p$  is the received  $Nr \times 1$  signal on the  $p$ -th subcarrier,  $\mathbf{x}^p$  is the  $t \times 1$  transmit signal vector and  $\mathbf{n}^p$  is the  $Nr \times 1$  thermal noise vector on the  $p$ -th subcarrier of each receive antenna. We can write the channel matrix on the  $p$ -th subcarrier as

$$\mathbf{H}^p = [\mathbf{H}_1^{pT} \mathbf{H}_2^{pT} \dots \mathbf{H}_N^{pT}]^T. \quad (2)$$

Following the CBST approach we obtain  $\mathbf{x}^p$  as follows

$$\mathbf{x}^p = \sum_{j=1}^r b_{1j}^p \mathbf{w}_{1j}^p + \sum_{j=1}^r b_{2j}^p \mathbf{w}_{2j}^p + \dots + \sum_{j=1}^r b_{Nj}^p \mathbf{w}_{Nj}^p = \mathbf{W}^p \mathbf{b}^p, \quad (3)$$

where  $b_{ij}^p$  represents the  $j$ -th symbol for user  $i$  transmitted with power  $P_{ij}^p$  on the  $p$ -th subcarrier and  $\mathbf{w}_{ij}^p = [w_{ij}^{p,1}, \dots, w_{ij}^{p,t}]$  are the precoding vectors calculated through BD as in [2] to guarantee

$$\mathbf{H}_i^p [\mathbf{w}_{k1}^p, \mathbf{w}_{k2}^p, \dots, \mathbf{w}_{kr}^p] = \begin{cases} \mathbf{0} & \text{if } i \neq k \\ \mathbf{U}_i^p \mathbf{S}_i^p & \text{if } i = k \end{cases}, \quad (4)$$

where  $\mathbf{0}$  is an all zero matrix of dimensions  $r \times r$ ,  $\mathbf{U}_i^p$  is a  $r \times r$  unitary matrix and  $\mathbf{S}_i^p$  is defined as

$$\mathbf{S}_i^p = \text{diag}\{(\lambda_{i1}^p)^{1/2}, (\lambda_{i2}^p)^{1/2}, \dots, (\lambda_{ir}^p)^{1/2}\}. \quad (5)$$

Then, the received signal on the  $p$ -th subcarrier can be expressed as

$$\mathbf{y}^p = \begin{bmatrix} \mathbf{U}_1^p \mathbf{S}_1^p & \mathbf{0} & \dots & \mathbf{0} \\ \mathbf{0} & \mathbf{U}_2^p \mathbf{S}_2^p & \dots & \mathbf{0} \\ \vdots & \vdots & \ddots & \vdots \\ \mathbf{0} & \mathbf{0} & \dots & \mathbf{U}_N^p \mathbf{S}_N^p \end{bmatrix} \mathbf{b}^p + \mathbf{n}^p. \quad (6)$$

Thus, each user may independently rotate and decouple the different streams by multiplying the received signal with the  $\mathbf{U}_i^{pH}$  unitary matrix. Note that the noise remains white with the same covariance because of the unitary transformation. Hence, under this strategy, the overall system boils down to a set of parallel non-interfering channels.

For simplicity, throughout this paper an equal power allocation  $\rho = P_{ij}^p = P/N \forall i = 1, \dots, N, j = 1, \dots, r, p = 1, \dots, N_{ofdm}$  is assumed. According to (4) and assuming the same complex Gaussian noise with variance  $\sigma^2$  in each receive antenna, the achievable rate of the  $i$ -th user can be written as

$$R_i = \sum_{p=1}^{N_{ofdm}} \log_2 \det [\mathbf{I}_r + \frac{\rho}{\sigma^2} \mathbf{W}_i^{pH} \mathbf{H}_i^{pH} \mathbf{H}_i^p \mathbf{W}_i^p]. \quad (7)$$

## 2.1. Achievable throughput for imperfect CSIT

So far, a perfect CSIT has been assumed and the interference could be completely avoided. Under imperfect CSIT an interference term appears in the achievable rate. The instantaneous channel for the  $i$ -th user is denoted  $\mathbf{H}_i$  and the estimated channel after the feedback stage is denoted as  $\widehat{\mathbf{H}}_i$ . To distinguish the precoding matrices obtained under the system estimated channel  $\widehat{\mathbf{H}}$  we denote these matrices as  $\widehat{\mathbf{W}}_1, \dots, \widehat{\mathbf{W}}_N$ . Thus, the received signal on the  $p$ -th subcarrier is given by

$$\mathbf{y}_i^p = \mathbf{H}_i^p \widehat{\mathbf{W}}_i^p \mathbf{b}_i^p + \sum_{\substack{k=1 \\ k \neq i}}^N \mathbf{H}_i^p \widehat{\mathbf{W}}_k^p \mathbf{b}_k^p + \mathbf{n}_i^p. \quad (8)$$

For imperfect CSIT [4] the user rate can be written as

$$R_i = \sum_{p=1}^{N_{ofdm}} \log_2 \frac{\det [\mathbf{I}_r + \frac{\rho}{\sigma^2} \sum_{k=1}^N \widehat{\mathbf{W}}_i^{pH} \mathbf{H}_i^{pH} \mathbf{H}_i^p \widehat{\mathbf{W}}_i^p]}{\det [\mathbf{I}_r + \sum_{\substack{k=1 \\ k \neq i}}^N \frac{\rho}{\sigma^2} \widehat{\mathbf{W}}_k^{pH} \mathbf{H}_i^{pH} \mathbf{H}_i^p \widehat{\mathbf{W}}_k^p]}. \quad (9)$$

## 2.2. Zero forcing vs. Block diagonalization

Under the assumption that the receive antennas can be treated independently, the BD technique collapses to ZF where the precoding matrices are calculated as  $\mathbf{W}_{ZF}^p = \mathbf{H}^{pH} (\mathbf{H}^{pH} \mathbf{H}^{p*H})^{-1}$  and the achievable rate of each user is given by the sum of the rates achieved in each receiver input. Therefore it is interesting to compare the performance of both techniques in a real implementation. According to [4] the rate gap between BD and ZF with perfect CSIT, which would be slightly greater under limited feedback, is given by

$$R_{gap} = N \log_2(e) \sum_{j=1}^r \frac{r-j}{j}. \quad (10)$$

## 3. MEASUREMENT SET-UP

The testbed [8] configuration is shown in Figure 1. The transmit base station is equipped with  $t = 4$  antennas which serves  $N = 2$  users equipped with  $r = 2$  antennas each one. Therefore four data streams, two per user, are sent simultaneously using BD. Both transmitter and users are located in a lecture room at the University of Santander. The users are separated around six meters away from the base station with direct line of sight. Finally the system parameters are shown in Table 1.

Figure 2 shows the transmit side as a mixture of software and hardware parts. The dashed lines indicate the blocks that only are employed in a corresponding phase of the data transmission frame. A LTE 1/3 encoder is only employed if turbo-coding scheme is selected. On the other hand, BD precoder block is only used during the simultaneous transmission phase of the data transmission stage. Apart from that, the following steps are carried out

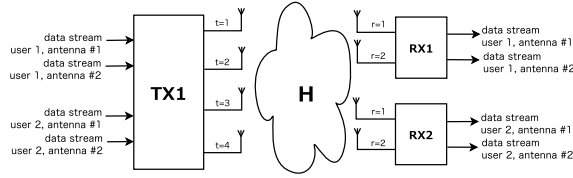


Fig. 1. Measurement configuration.

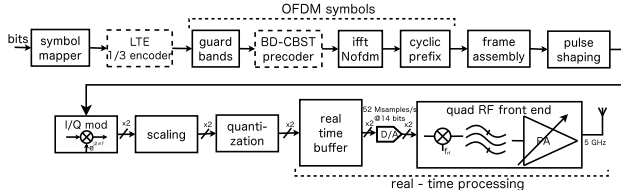


Fig. 2. Block diagram of hardware and software elements at transmit side.

- Source bits are mapped to a BPSK, QPSK, 16QAM, 32QAM or 64QAM constellation with one symbol per subcarrier. Pilot symbols are always mapped to QPSK.
- The OFDM symbols are generated in the following blocks.
- A Pseudo-Noise (PN) sequence is added as a preamble for synchronization in the frame assembly block.
- The whole signal is up-sampled and the resulting signal is pulse-shaped employing a square root-raised cosine filter with 40% roll off, leading to a signal bandwidth of 9.1 MHz (Digital-to-Analog Converters (DACs) sampling frequency is set to 52 MHz).
- The signal is properly scaled and quantized according to the 14 bits DAC resolution.
- The signal is stored in the real time buffers waiting to be transmitted. Once all signals are ready, they are sent to the RF front-end and transmitted at the desired RF center frequency.

The receive side is described in Figure 3. In this case the dashed lines indicate the blocks which are used in BD and turbo coding schemes respectively. Additionally a new dashed block called channel estimation appears. In this section, the received pilots are used to estimate the  $h_{i,j}^p$ . SISO channels which generate the set of  $N_{ofdm}$   $\mathbf{H}^p$  MIMO channel matrices. Finally, the following steps are performed

- The RF front-end downconverts the received signals generating the corresponding in-phase (I) and quadrature (Q) analog signals which are digitalized by the 52 MHz ADCs. Finally they are stored in the real time buffers.

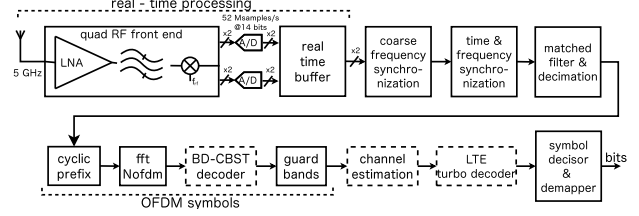


Fig. 3. Block diagram of hardware and software elements at each receive node.

Table 1. System parameters

Parameter	Value
Signal bandwidth	9.1 MHz
RF carrier	5600 MHz
Number of subcarriers	128
Subcarrier spacing	50.68 KHz
Data subcarriers	96
Null/Guard subcarriers	32
Cyclic prefix	1/8 of the OFDM symbol length
Frequency sampling	52 Msamples/sec
Sampling rate	8 samples/symbol

- Next two blocks perform the coarse frequency and time synchronization.
- Once the signals are synchronized, they are filtered and decimated according to the defined number of samples per symbol.
- The OFDM symbols are demodulated according to the system parameters. Remark that the receiver BD decoder weights  $U_i^p H$  are updated based on the last received data.
- Finally a symbol decisor is applied in each symbol followed by a demapper.

#### 4. MEASUREMENT METHODOLOGY

Figure 4 shows the frame structure designed for the proposed testbed. This frame is composed by the following stages:

- **Training stage:** a sequential transmission scheme is used during this section. Each transmit antenna sends an interference free training signal which is received by the users. Therefore the receivers can obtain the channel characterization of each transmit antenna. The training frame is composed by a PN sequence for synchronization and a known OFDM pilot (PLT) symbol. Once all training signals have been acquired, the following steps are carried out:

1. The  $16 \times N_{ofdm}$  Single Input Single Output (SISO) channels are estimated in each subcarrier. Following the  $N_{ofdm}$  MIMO channels  $\hat{\mathbf{H}}^p$  are constructed.
2. The set of BD precoders  $\hat{\mathbf{W}}^p$  and decoders  $\hat{\mathbf{U}}^p$  are calculated in each subcarrier using the previous MIMO-OFDM channel measurements.
3. The noise variance is estimated during the non-transmission period.
4. After this process, the corresponding OFDM signals are generated and transmitted assuming equal power transmission in each antenna.

All these operations take around five seconds to be completed.

- **Data transmission stage:** The signals are generated according with the BD precoders obtained in the previous stage. Given that our approach considers two possibilities, ZF and BD, the data transmission stage is carried out twice. This stage comprises two phases:

1. **Simultaneous transmission:** All transmit antennas send data streams to receivers simultaneously on the wireless channel.
2. **Sequential transmission:** A time division multiple access (TDMA) approach is employed in this phase. Hence, each receive input obtains a data stream free of interference at the price of wasting space/time dimensions. On the other hand, TDMA does not require CSIT knowledge. Therefore, the obtained results are useful for comparison when CSIT is not available. Note that the pilot symbols are transmitted again for the purpose of obtain the instantaneous channel matrix  $\mathbf{H}$ .

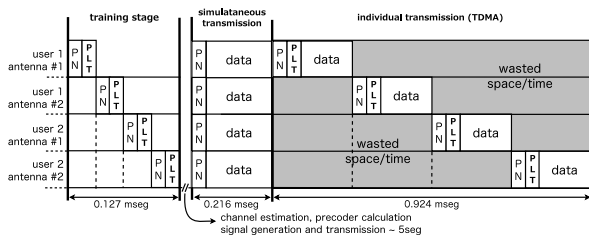


**Fig. 4.** Frame structure designed for the experimental validation of block diagonalization schemes.

The measurement process is carried out for constellations from BPSK to 64-QAM with the aim to obtain the sum throughput of the system. The presented results show the bit error rate (BER) performance for each constellation which determine the sum rate. Hence, a large number of executions

are necessary to obtain an accurate performance analysis. Around 1000 measurements are carried out where the data frame is formed by 10 OFDM symbols. With the exception of the use of turbo codes, where 10000 measurements have been realized with the aim to obtain BER results below  $10^{-6}$ .

## 5. RESULTS

The theoretic achievable rates according with the testbed channel measurements are shown in Figure 5. We can see that a performance about 6 bits/sec/Hz is almost guaranteed for ZF while this rate is about 9.2 bit/sec/Hz for BD. This difference of 3.2 bits/sec/Hz is consistent with the rate gap between these techniques. For the 2-user equipped with 2 antennas case, this gap is  $2 \log_2(e) \approx 2.88$  with perfect CSIT and even greater under imperfect CSIT conditions.

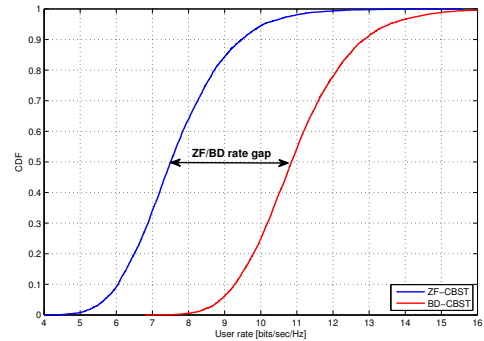


**Fig. 5.** CDFs of the theoretic achievable rate for ZF and BD.

The performance in each receive input for BD is plotted in Figure 6. Note that the BER of the second antennas are always greater than the first antennas. This is because in BD  $\lambda_{i,j} \geq \lambda_{i,j+1}$ , hence the first parallel channel  $\lambda_{i,1}$  is always stronger than  $\lambda_{i,2}$ . On the other hand, these results have been obtained under an equal power allocation approach and the same constellations have been used in all streams at the same time. Therefore it would be possible to improve the achieved results employing bit-loading algorithms and more complex power allocation strategies.

Figure 7 shows a comparison of the system BER vs sum throughput for BD, ZF and TDMA techniques. From this figure we can conclude that BD is able to achieve higher sum-rate than TDMA with a lower BER, even when bit-loading or power allocation techniques are not applied. It is also interesting to analyze the ZF case, which is characterized by a high BER. This is usually due to one or more receive inputs whose ZF features is very low. Therefore it would be necessary to assign zero transmit power to these data streams with the aim to improve the system performance. Remark that the strong point of BD regarding ZF, is that it obtains better performance under imperfect CSIT due to the dimensionality advantage.

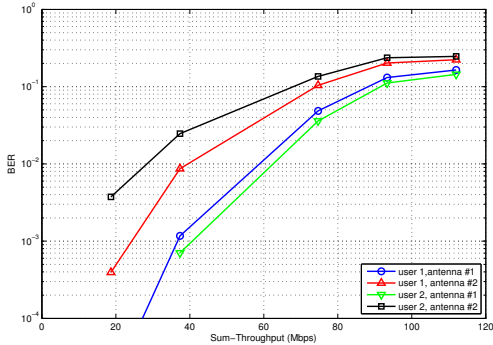


**Fig. 6.** User BER vs system sum rate for BD without channel coding.

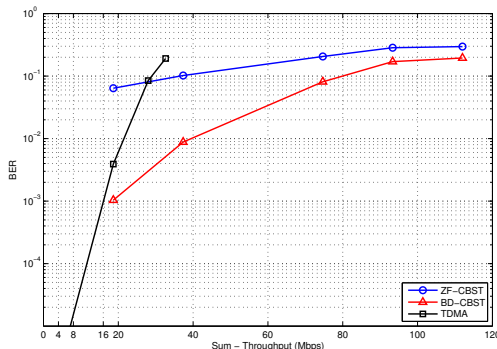


**Fig. 7.** Mean system BER vs sum rate for BD, ZF, and TDMA transmission without channel coding.

Figure 8 shows the results when a turbo code with rate 1/3 is applied for BD and ZF. Since this approach allows to obtain results close to the capacity, the obtained BER is significantly lower than without coding. The estimated channels obtained in this simulation have been employed to calculate the theoretic rates shown in Figure 5. Remark that horizontal axis corresponds to the spectral efficiency in bits per symbol. Thus, it is possible to check that bit errors commence to appear when the transmission scheme use more bits per symbol than the theoretic achievable rate. These values correspond to 4.5 and 8 bits per symbol for ZF and BD respectively.

## 6. CONCLUSIONS

In this paper we have presented the performance of BD in a real implementation using an indoor MIMO-OFDM testbed. First of all, according to the measured channels and a previous offline evaluation, the theoretic achievable rates are shown. After that, the performance in BER terms regarding the achieved sum rate is presented concluding that BD is able

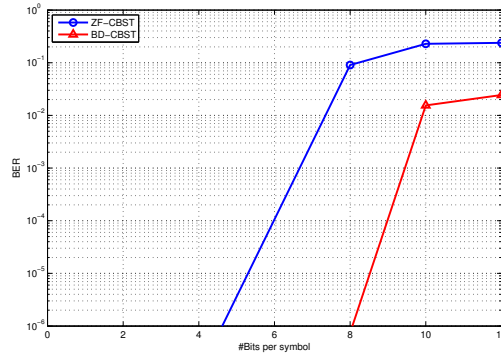


**Fig. 8.** Mean system BER vs sum rate for BD and ZF transmission with channel coding.

to achieve a higher sum-throughputs than ZF or TDMA. Finally the use of turbo codes with rate 1/3 allows us to achieve sum-throughputs close to the theoretical results.

## 7. REFERENCES

- [1] Lai-U Choi and R.D. Murch, "A transmit preprocessing technique for multiuser mimo systems using a decomposition approach," *Wireless Communications, IEEE Transactions on*, vol. 3, no. 1, pp. 20–24, Jan. 2004.
- [2] Q.H. Spencer, A.L. Swindlehurst, and M. Haardt, "Zero-forcing methods for downlink spatial multiplexing in multiuser mimo channels," *Signal Processing, IEEE Transactions on*, vol. 52, no. 2, pp. 461–471, Feb. 2004.
- [3] V.R. Cadambe and S.A. Jafar, "Interference alignment and spatial degrees of freedom for the k user interference channel," in *Communications, 2008. ICC '08. IEEE International Conference on*, May. 2008, pp. 971–975.
- [4] N. Ravindran and N. Jindal, "Limited feedback-based block diagonalization for the mimo broadcast channel," *Selected Areas in Communications, IEEE Journal on*, vol. 26, no. 8, pp. 1473–1482, Oct. 2008.
- [5] O. El Ayach, S.W. Peters, and R.W. Heath, "The feasibility of interference alignment over measured mimo-ofdm channels," *Vehicular Technology, IEEE Transactions on*, vol. 59, no. 9, pp. 4309–4321, Nov. 2010.
- [6] O. González, D. Ramírez, I. Santamaría, J.A. García-Naya, and L. Castedo, "Experimental validation of interference alignment techniques using a multiuser mimo testbed," in *Smart Antennas (WSA), 2011 International ITG Workshop on*, Feb. 2011.
- [7] H. Vlad Balan, R. Rogalin, Michaloliakos. A, Psounis. K, and Caire. G, "Achieving high data rates in a distributed mimo system," in *in Proceedings of ACM MOBICOM*, Aug. 2012.
- [8] L. Vielva, J. Via, J. Gutiérrez, O. Gonzalez, J. Ibáñez, and I. Santamaría, "Building a web platform for learning advanced digital communications using a mimo testbed," in *Acoustics Speech and Signal Processing (ICASSP), 2010 IEEE International Conference on*, March. 2010, pp. 2942–2945.